DOI: 10.1021/ma902317k

Macromolecules
ARTICLE

Electrochemical Synthesis of Polyaniline Nanobelts with Predominant Electrochemical Performances

Gao-Ren Li,* Zhan-Ping Feng, Jin-Hui Zhong, Zi-Long Wang, and Ye-Xiang Tong*

MOE Laboratory of Bioinorganic and Synthetic Chemistry/School of Chemistry and Chemical Engineering/ Institute of Optoelectronic and Functional Composite Materials, Sun Yat-Sen University, Guangzhou 510275, P. R. China

Received October 19, 2009; Revised Manuscript Received January 25, 2010

ABSTRACT: Polyaniline (PANI) as one of most promising conducting polymers has attracted much attention because of its low cost, superior electrochemical performance, distinguishable electrical properties, mechanical flexibility, and relative ease of processing. In this article, we explored a novel route to prepare PANI nanobelts directly onto conducting substrates by electrodeposition, which represents a facile synthetic method for the synthesis of high quality samples with excellent electrical contact to a substrate, which is critical for further supercapacitor testing. The products were characterized by scanning electron microscopy (SEM), powder X-ray diffraction analysis (XRD), and Fourier transform infrared (FTIR) analysis. These prepared PANI nanobelts were found to have a large surface area, which promotes remarkable enhancement in the performance of supercapacitors. The PANI electrodes composed of nanobelts showed a high specific capacitance (SC) value of 873 Fg^{1-} at 10 mVs^{-1} and high stability over 1000 cycles. The results of electrochemical measurements show that these PANI nanobelts have a potential application as high-performance supercapacitor electrode material.

1. Introduction

Because of the depleting fossil fuels, developing alternative energy conversion or storage devices with high power and energy densities is under serious consideration. At present, supercapacitors, fuel cells, and lithium ion batteries are strongly considered as major contenders for power source applications.[1−3] Recently, the efforts in developing better supercapacitors have gained importance because of their high power and energy density, which is considered to be an ideal power source for applications such as digital communication, electric vehicles, and so on.[4] Various materials have been investigated for supercapacitors including (i) transition-metal oxides, (ii) conducting polymers, and (iii) carboneous materials. Conducting polymers have been regarded as promising pseudocapacitive materials because the kinetics of the charge−discharge processes of polymers with suitable morphology is fast, and they can generally be produced at lower cost than noble metal oxides and are comparable to that of activated carbons.[5] Among the various conducting polymers, PANI has been studied extensively because it is inexpensive, easy to synthesize, and has good environmental stability, redox reversibility, and electrical conductivity.[6] Different methods have been used to synthesize PANI, such as emulsions,[7] template synthesis,[8] self-assembly,[9] and interfacial polymerization.[10] However, large amounts of surfactants are required in the above methods, and this will make PANI difficult to attach the substrate without involving large contact resistance.[11] The adherent films of PANI on the substrate, which can be directly used for electrochemical studies, can be easily prepared by the electrochemical deposition route.[12] The electrochemical synthesis of PANI shows a simple and low-cost route.

Recently, along with the fast development of nanoscience and nanotechnology, more and more attention has been attracted by the controlled synthesis of PANI nanostructures to find potential applications in supercapacitor.[13] The PANI materials with nanostructures will give better electrochemical performances because of their distinctive characteristics of conducting pathways and surface interactions. Up to now, PANI nanowires,[14] nanorods,[15] nanotubes,[16] nanoparticles,[17] nanofibers,[18] and other nanostructures[19] have been widely studied with the expectation that such materials will possess the advantages of both low-dimensional systems and organic conductors. However, PANI nanobelts as important 1D nanostructures are rarely reported.[20] In this article, we report a simple way to prepare well-controlled PANI nanobelts via a template-free electrochemical method by controlling the appropriate deposition potential. The following two points were desirable and significant in this study: (i) developing a facile electrochemical route for the preparation of PANI nanobelts directly onto conducting substrates, which represents a facile synthetic method for the synthesis of high quality samples with excellent electrical contact to a substrate (this is critical for further supercapacitor testing) and (ii) exploring the predominant electrochemical properties of PANI nanobelts, which will provide experimental support for scientists to find their potential applications in the supercapacitros. To the best of our knowledge, up to now, there is almost no report on the electrochemical properties of PANI nanobelts. These prepared PANI nanobelts are characterized by SEM, XRD, FTIR, and Raman spectra, and they are expected to make a significant contribution to the advancement of electrochemical pseudocapacitor technology because of their high pseudocapacitive behavior and electrochemical stability.

2. Experimental Section

The PANI nanobelts were electrodeposited using HDV-7C transistor potentiostatic apparatus connected to a simple three-electrode electrochemical cell. The three-electrode configuration contains Ti sheet as a working electrode, a graphite electrode as

*Corresponding author. E-mail: ligaoren@mail.sysu.edu.cn (G.-R.L.); chedhx@mail.sysu.edu.cn (Y.-X.T.).

 Published on Web 02/12/2010

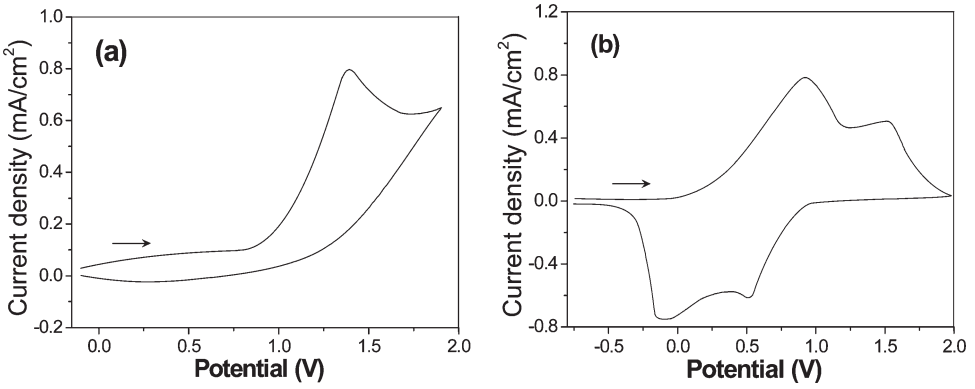

Figure 1. Cyclic voltammograms of (a) Pt electrode in solution of 0.05 M aniline + 1.0 M H_2SO_4 and (b) the prepared PANI films in neutral 0.1 M TBAP solution.

Scheme 1. Electrochemical Formation Process of PANI

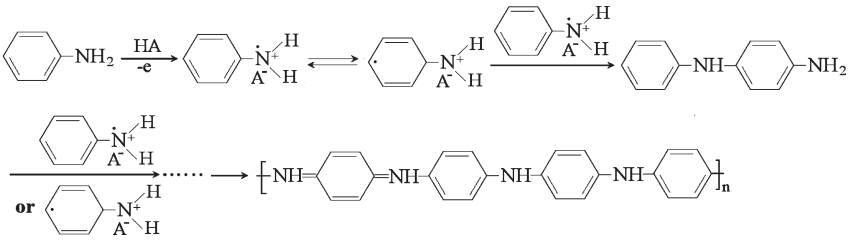

the counter electrode, and a saturated calomel electrode (SCE) as the reference electrode that was connected to the cell with a double salt bridge system. The electrodeposition was carried out in a solution of 0.1 M aniline (pH 5) by galvanostatic electrolysis with current density of 1.0 or 2.0 mA/cm^2 at room temperature. Before the electrodeposition, the substrate was polished by SiC abrasive paper from 300 to 800 grits. After it was dipped in HCl (5%) for 5 min, it was washed by distilled water and rinsed with acetone in ultrasonic bath before each experiment.

The surface morphologies of the obtained PANI nanobelts were observed by field emission scanning electron microscopy (FE-SEM, JSM-6330F). The obtained products were characterized by X-ray diffraction (XRD, PIGAKU, D/MAX 2200 VPC) to determine the deposit structures. Optical properties of PANI nanobelts were tested with infrared ray spectrometer (FT-IR, Nicolet 330). A Chi750B electrochemical workstation was used for the electrochemical measurements. The PANI nanobelts as electrodes were studied for redox supercapacitor applications in 1.0 M H_2SO_4 electrolyte (the loading is ~0.175 mg). The Pt sheet was used as a counter electrode, and the SCE was used as the reference electrode. The cyclic voltammetry experiments were performed between −0.25 and 0.75 V versus SCE at a scan rate of 10−250 mV/s.

3. Results and Discussion

The cyclic voltammogram was recorded for Pt electrode in solution of 0.05 M aniline +1.0 M H_2SO_4, as shown in Figure 1a. The potential was scanned from −0.15 to +2.0 V (versus SCE) at a rate of 40 mV/s. The anodic peak started around +0.83 V (versus SCE) can be attributed to electro-oxidation of aniline.[21] The peak potential is about +1.39 V. When the electrodeposition was carried out in a solution of 0.05 M aniline + 1.0 M H_2SO_4 at +1.50 V, the PANI films can be successfully prepared on the Ti substrate. The cyclic voltammogram of these prepared PANI films in neutral tetrabuthylammonium perchlorate (0.1 M TBAP) solution is shown in Figure 1b. Two broad oxidation and two reduction peaks are observed. The first oxidation peak at the potential of +0.92 V can be attributed to the formation of the leucoemeraldine cation radical from leucoemeraldine.[21] The reverse reduction process occurs with a peak potential of −0.12 V. The leucoemeraldine cation radical is further oxidized to emeraldine at the peak potential of +1.53 V with a corresponding cathodic peak at +0.51 V belonging to the reverse process.[21] The above results show that the PANI films can be successfully synthesized via electrochemical deposition route in a solution of 0.05 M aniline + 1.0 M H_2SO_4. Scheme 1 shows the electrochemical formation process of PANI.

Figure 2 shows a typical SEM image of the PANI thin films electrodeposited in solution of 0.1 M aniline (pH 5) with cathodic current density of 1 mA/cm^2 for 12 h at 70 °C. It shows the PANI nanobelts were successfully prepared. The average width of PANI nanobelts is ~2 μm, and the average thickness is ~50 nm. The length of PANI nanobelts can be 20 μm. To investigate the formation mechanism of PANI nanobelts, the growth process of PANI films is illustrated as follows. It is well-known that the electrochemical polymerization of aniline mainly involved two stages.[22] First, a compact granular layer of PANI is formed on the bare electrode in the initial stage. Second, PANI further grows and then forms a loosely bound open structure in the advanced stage. Furthermore, the electrochemical growth process of PANI is revealed to be similar to that of conventional growth of PANI.[23] Therefore, PANI nanobelts can be synthesized easily over a wide range of experimental parameters by electrochemical methods. This can be attributed to following reasons: (1) electrophilic substitution reaction mainly takes place at the *p*-position of aniline and (2) aniline oligomers have 1D structure. Scheme 2 (1) shows the formation process of PANI nanobelts. When the electrodeposition of PANI is carried out, a large number of PANI nodules will be formed on the surface of substrate in the initial stage. Then, these formed nodules will be further polymerized to form the longer molecular chain via the electrophilic substitution reaction at the *p*-position of aniline. Because the pH value of deposition solution is 5, the aniline radical cation with positive charge is formed, and accordingly, the electrophilic substitution reaction at the *p*-position will become easier. In addition, numerous aniline oligomers with 1D structure also exist in deposition solution, and they can also connect with these nodules. As a result, these nodules will be evolved to PANI nanobelts on the surface of the substrate. For the electrochemical

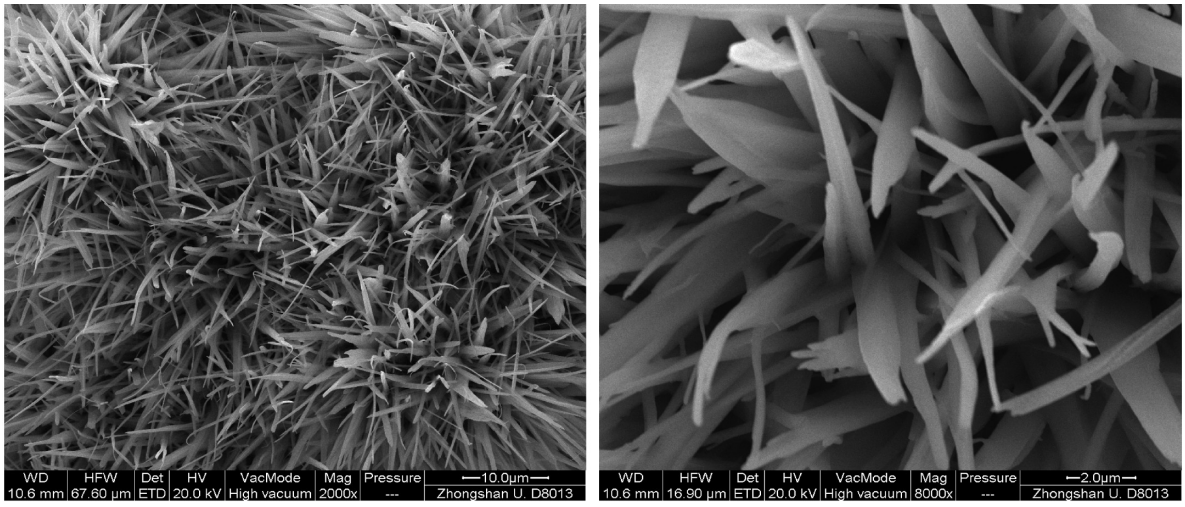

Figure 2. SEM images of PANI nanobelts electrodeposited in a solution of 0.1 M aniline solution (pH 5) with current density of 1 mA/cm^2 at 70 °C for 12 h. (a) 2000× and (b) 8000×.

Scheme 2. Schematic Illustration of the Formation Processes of (1) PANI Nanobelts and (2) PANI Nanospheres

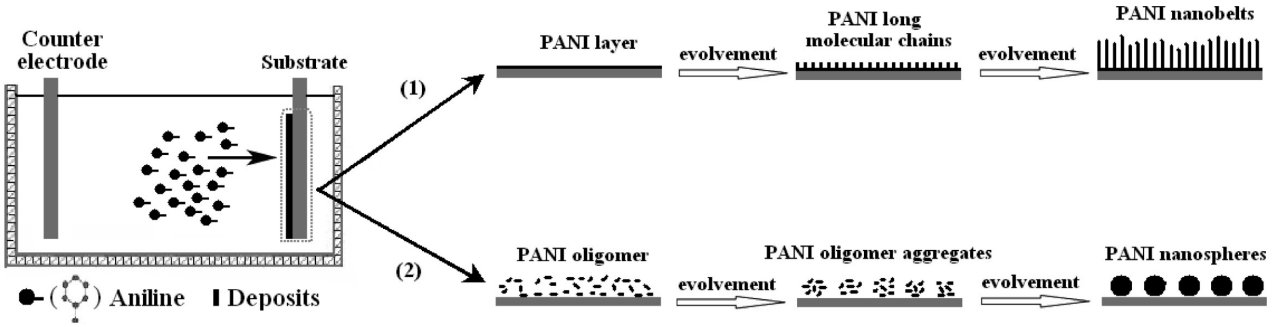

synthesis of PANI, many reports can be found in the literatures,[24] and usually, the PANI nanofibers, nanowires, or nanoparticles are prepared. However, in our article, PANI nanobelts are successfully synthesized, and this may be attributed to the special synthesis conditions in our article. The effects of current densities of electrodeposition on the morphologies are investigated in detail. When the electrodeposition was carried out with current density of 0.5 mA/cm^2 for 12 h, the PANI nanosheets were obtained, as shown in Figure S1 of the Supporting Information. The width of PANI nanosheets can be achieved to >20 μm. When the current density of electrodeposition was enhanced to be 2 mA/cm^2 for 12 h, the nanospheres were obtained, as shown in Figure 3. The average size of nanospheres is ~250 nm. When the current density was further enhanced to 5 mA/cm^2, the smaller nanoparticles were obtained, as shown in Figure S2 of the Supporting Information, and their sizes were ~150 nm. Therefore, the current density can obviously affect the polymerization or elongation rate of aniline, and accordingly, it will obviously affect the morphology of PANI. It is known that the polymerization of PANI occurred simultaneously with the decomposition, and a competition existed in them.[25] The conversion of PANI nanostructures from nanosheets to nanobelts and to nanospheres can be attributed to the decomposition of PANI. With the increasing of the current density, the decomposition of PANI became faster. PANI nanosheets were first converted to nanobelts. Then, PANI nanobelts were converted to PANI nanoparticles because of the formation of short molecular chains. The short molecular chains are easily evolved to PANI nanoparticles because they have lower surface energy. The formation process of PANI nanoparticles has been shown in Scheme 2 (2).

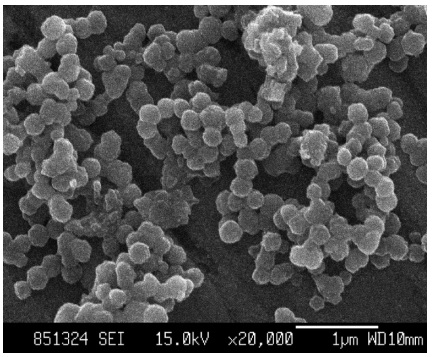

Figure 3. SEM image of PANI nanospheres electrodeposited in solution of 0.1 M aniline solution (pH 5) with current density of 2 mA/cm^2 at 70 °C for 12 h.

The solid-state properties of PANI deposits were investigated, and Figure 4 shows the XRD pattern of the prepared PANI nanobelts. A very broad peak centered at $2\theta = 21.3°$ was observed in the XRD pattern. This suggests that the nature of the nanowires is amorphous. Other Ti peaks come from the substrate. The structure of the PANI deposits was further characterized by Fourier transform infrared (FTIR) spectrum, and Figure 5 shows the typical FTIR spectrum of PANI nanobelts. The bands at 3434, 3356, and 3216 cm^{-1} represent N−H stretching modes. The bands at 3144 and 3032 cm^{-1} can be assigned to aromatic C−H stretching modes. The characteristic absorbances at about 1601 and 1494 cm^{-1} indicate the signature of the PANI backbone due to the stretching modes of the

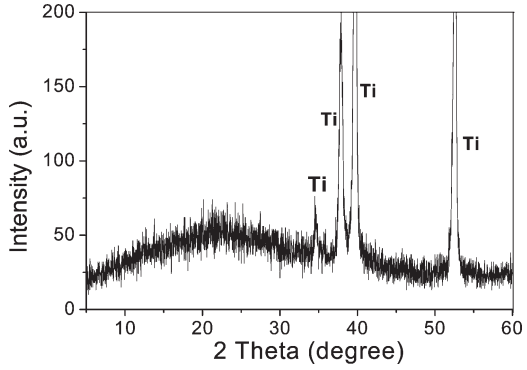

Figure 4. XRD pattern of PANI nanobelts electrodeposited in solution of 0.1 M aniline solution (pH 5) with current density of 1 mA/cm^2 at 70 °C for 12 h.

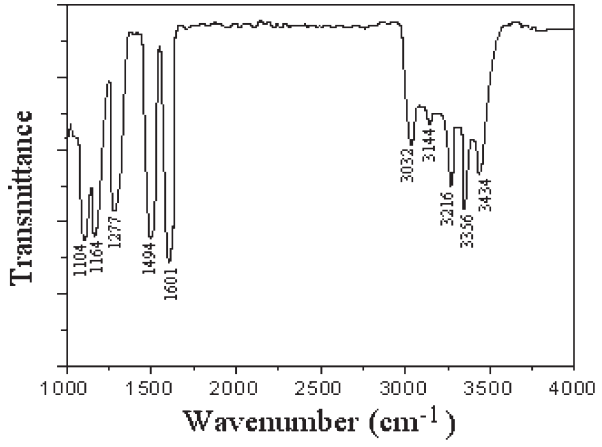

Figure 5. FTIR spectrum of PANI nanobelts electrodeposited in solution of 0.1 M aniline solution (pH 5) with current density of 1 mA/cm^2 at 70 °C for 12 h.

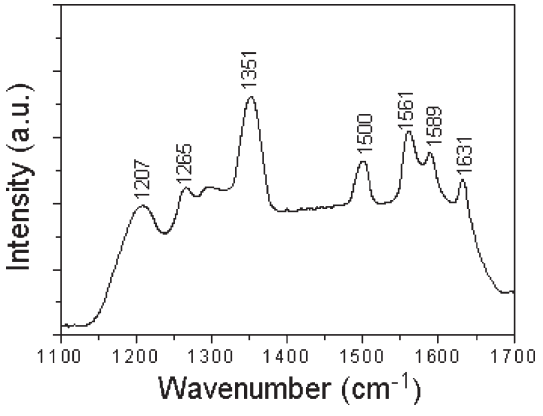

Figure 6. Raman spectrum of PANI nanobelts electrodeposited in solution of 0.1 M aniline solution (pH 5) with current density of 1 mA/cm^2 at 70 °C for 12 h.

protonated quinoid ring and the benzenoid ring. The band at 1277 can be assigned to the C−N stretching mode in a secondary aromatic amine. Two bands at 1164 and 1104 cm^{-1} correspond to an aromatic C−H in-plane bending mode. Therefore, the results of FTIR spectrum demonstrated the PANI were prepared and existed in the conducting emeraldine form.

The Raman spectrum of PANI nanobelts was shown in Figure 6. The bands at 1631, 1589, and 1561 cm^{-1} correspond to the C−C deformation bands of semiquinone rings. The peak at ~1500 cm^{-1} is characteristic of the N−H bending deformation

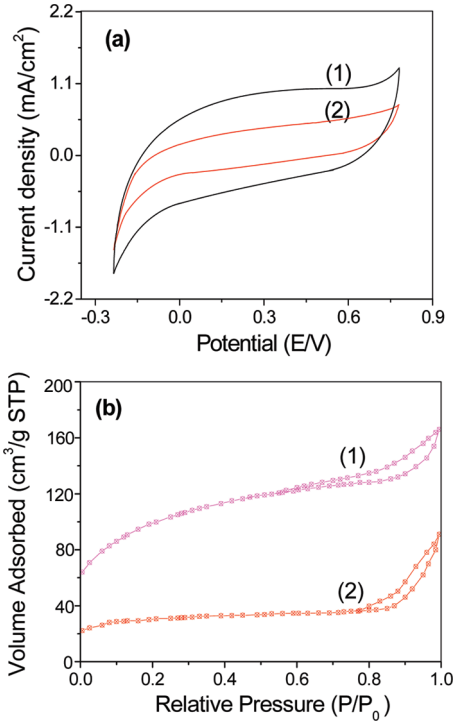

Figure 7. (a) CV of PANI nanobelts in solution of 1.0 mol/L H_2SO_4 aqueous solution at 10 mV/s and (b) N_2 adsorption−desorption isotherms of (1) PANI nanobelts and (2) PANI nanospheres.

band of the protonated amine. The band at 1350 cm^{-1} can be assigned the C−N$^{\bullet+}$ stretching mode of the delocalized polaronic charge carriers. In particular, it should be noted that the strong intensity of this band suggests high concentration of C−N$^{\bullet+}$ stretching mode. The band at 1265 cm^{-1} corresponds to the C−N stretching mode of the polaronic units. In addition, a broadband at 1207 cm^{-1} is clearly observed, and it may be attributed to the coalition of the bands at 1221 and 1171 cm^{-1}. Therefore, this band shows the existence of the semiquinone structure and the C−N stretching mode.[26]

The electrochemical performance of PANI nanobelt electrodes was investigated by means of CVs in 0.1 M H_2SO_4 electrolyte solution at a scan rate of 10 mVs^{-1}. The representative CV of PANI nanobelts in the potential range of −0.24 to 0.78 V versus SCE is shown in Figure 7a. The redox insertion reaction originated from 3D absorption of electroactive species into the solid PANI. The near-rectangular-shaped CV and high overall current suggest the highly capacitive behavior of the polyaniline nanobelts. The SC value of PANI nanobelt electrodes at 10 mVs^{-1} is calculated to be ~873 F/g. However, for PANI nanoparticles, the SC value is only ~382 F/g. Therefore, the PANI nanobelt electrodes showed a much larger SC value than that of PANI nanospheres. On the basis that these PANI nanobelts and nanospheres synthesized under different conditions have the same chemical structures, this SC difference may be attributed to the availability of larger surface area for redox reactions in PANI nanobelts than nanospheres. To examine the surface properties of the synthesized PANI nanobelts and nanospheres, we characterized the porosity by nitrogen sorption analysis using standard Brunauer−Emmett−Teller (BET) techniques. The nitrogen adsorption and desorption isotherms of PANI nanobelts, bugle-like nanostructures, and nanospheres are shown in Figure 7b (1) and (2), respectively. The PANI nanobelts and nanospheres show the specific surface areas of 343 and 106 m^2/g, respectively. Thus, the specific surface area of PANI nanobelts increased up to ~3.0 times compared with that of nanospheres. Therefore, the redox reactions in PANI nanobelt electrodes will be much faster

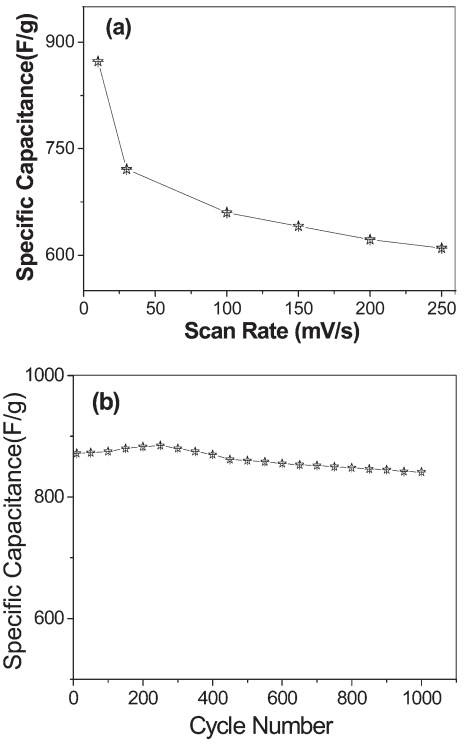

Figure 8. (a) Specific capacitance as a function of the scan rate. (b) Specific capacitance as a function of the cycle number at 10 mV/s.

because of their larger available surface area. The SC value of 873 F/g of PANI nanobelts reported here is also much bigger than those of PANI nanofibers (122 Fg^{1-})[27] and porous nanowires (700 F/g).[28]

The dependency of the calculated specific capacitance (SC) values of PANI nanobelts on the scan rate is shown in Figure 8a. When the scan rate is 10 mV s^{-1}, the SC value of 873 F g^{-1} was obtained, whereas the SC value of 622 F g^{-1} was obtained at the high scan rate of 200 mV s^{-1}. It is accepted that at a low scan rate, the presence of inner active sites, which undergo the redox transitions completely, can lead to produce SC value superior to that at high scan rate because of the diffusion effect of proton within the electrode.[29] The decrease is ~30% in the SC when the scan rate was increased from 10 to 250 mV s^{-1}. However, for metal oxides, the SC decrease will be 50−80% when the scan rate was increased from 10 to 250 mV s^{-1}.[30] Figure 8b shows the cyclic stability of PANI nanobelt electrodes at the sweep rate of 10 mV s^{-1}. During the initial cycles, it is found that there is a gradual increase in the SC value from 837 to 885 Fg^{1-} in the first 300 cycles. A little decrease is observed from 300 to 550 cycles, and thereafter, it remains fairly constant up to 1000 cycles. The decrease in the SC was ~3.5% in 1000 cycles for PANI nanobelts. Therefore, the PANI nanobelt electrodes show high stability and retain its electrochemical capacitance property over 1000 cycles.

4. Conclusions

In summary, PANI nanobelts were successfully synthesized via a simple, rapid, and efficient electrochemical route. Compared with PANI nanospheres, these prepared PANI nanobelts show much larger surface areas, which can promote remarkable enhancement in the performance of supercapacitors. The PANI nanobelt electrodes show a high SC value of 873 Fg^{1-} at 10 mVs^{-1}, which is much bigger than that of PANI nanosphere electrodes. These prepared PANI nanobelt electrodes also show high stability and retain its electrochemical capacitance property over a large number of cycles. The high SC and good cycle ability of PANI nanobelt electrode coupled to the low cost and environmentally benign nature may make them attractive for supercapacitor applications. Herein, the reported synthesis method can be extended to the synthesis of other conducting polymer nanobelts.

Acknowledgment. This work was supported by NSFC (20603048, 20873184, and 90923008), Guangdong Province (2008B010600040 and 9251027501000002), and Sun Yat-Sen University (09lgpy17).

Supporting Information Available: SEM images of PANI nanosheets and nanoparticles. This material is available free of charge via the Internet at http://pubs.acs.org.

References and Notes

(1) Hu, C.-C.; Chang, K.-H.; Lin, M.-C.; Wu, Y.-T. *Nano Lett*. **2006**, *6*, 2690–2695.
(2) Kim, E.; Weck, P. F.; Balakrishnan, N.; Bae, C. *J. Phys. Chem. B* **2008**, *112*, 3283–3286.
(3) Xiao, J.; Chernova, N. A.; Stanley Whittingham, M. *Chem. Mater*. **2008**, *20*, 7454–7464.
(4) (a) Athouel, L.; Moser, F.; Dugas, R.; Crosnier, O.; Belanger, D.; Brousse, T. *J. Phys. Chem. C* **2008**, *112*, 7270–7277. (b) Selvan, R. K.; Perelshtein, I.; Perkas, N.; Gedanken, A. *J. Phys. Chem. C* **2008**, *112*, 1825–1830. (c) Suppes, G. M.; Deore, B. A.; Freund, M. S. *Langmuir* **2008**, *24*, 1064–1069. (d) Ryu, K. S.; Jeong, S. K.; Joo, J.; Kim, K. M. *J. Phys. Chem. B* **2007**, *111*, 731–739. (e) Hulicova, D.; Kodama, M.; Hatori, H. *Chem. Mater*. **2006**, *18*, 2318–2326. (f) Zhou, C.; Kumar, S.; Doyle, C. D.; Tour, J. M. *Chem. Mater*. **2005**, *17*, 1997–2002.
(5) (a) Arbizzani, C.; Mastragostino, M.; Meneghello, L.; Paraventi, R. *Adv. Mater*. **1996**, *8*, 331–334. (b) *The Application of Electroactive Polymers*; Scrosati, B., Ed.; Chapman & Hall: London, 1993. (c) Ryu, K. S.; Jeong, S. K.; Joo, J.; Kim, K. M. *J. Phys. Chem. B* **2007**, *111*, 731–739. (d) Suppes, G. M.; Deore, B. A.; Freund, M. S. *Langmuir* **2008**, *24*, 1064–1069. (e) Liu, F.-J. *J. Power Sources* **2008**, *182*, 383–388.
(6) (a) Jang, J.; Bae, J.; Choi, M.; Yoon, S.-H. *Carbon* **2005**, *43*, 2730–2736. (b) Mi, H.; Zhang, X.; Ye, X.; Yang, S. *J. Power Sources* **2008**, *176*, 403–409. (c) Sivakkumar, S. R.; Kim, W. J.; Choi, J.-A.; MacFarlane, D. R.; Forsyth, M.; Kim, D.-W. *J. Power Sources* **2007**, *171*, 1062–1068. (d) Mi, H.; Zhang, X.; An, S.; Ye, X.; Yang, S. *Electrochem. Commun*. **2007**, *9*, 2859–2862. (e) Ryu, K. S.; Kim, K. M.; Park, N.-G.; Park, Y. J.; Chang, S. H. *J. Power Sources* **2002**, *103*, 305–309. (f) Park, J. H.; Park, O O. *J. Power Sources* **2002**, *111*, 185–190.
(7) Wei, Z.; Wan, M. *Adv. Mater*. **2002**, *14*, 1314–1317.
(8) Niu, Z.; Yang, Z.; Hu, Z.; Lu, Y.; Han, C. C. *Adv. Funct. Mater*. **2003**, *13*, 949–954.
(9) Qiu, H.; Wan, M.; Matthews, B.; Dai, L. *Macromolecules* **2001**, *34*, 675–680.
(10) Huang, J.; Kaner, R. B. *J. Am. Chem. Soc*. **2004**, *126*, 851–855.
(11) Gupta, V.; Miura, N. *Mater. Lett*. **2006**, *60*, 1466–1469.
(12) Mondal, S. K.; Barai, K.; Munichandraiah, N. *Electrochim. Acta* **2007**, *52*, 3258–3264.
(13) (a) Sivakkumar, S. R.; Kim, W. J.; Choi, J.-A.; MacFarlane, D. R.; Forsyth, M.; Kim, D.-W. *J. Power Sources* **2007**, *171*, 1062–1068. (b) Gupta, V.; Miura, N. *Mater. Lett*. **2006**, *60*, 1466–1469. (c) Amarnath, C. A.; Chang, J. H.; Kim, D.; Mane, R. S.; Han, S.-H.; Sohn, D. *Mater. Chem. Phys*. **2009**, *113*, 14–17.
(14) (a) Ma, Y. F.; Zhang, J. M.; Zhang, G. J.; He, H. X. *J. Am. Chem. Soc*. **2004**, *126*, 7097. (b) Li, G.; Jiang, L.; Peng, H. *Macromolecules* **2007**, *40*, 7890–7894. (c) Li, G.; Zhang, Z. *Macromolecules* **2004**, *37*, 2683–2685. (d) Qiu, H.; Zhai, J.; Li, S.; Jiang, L.; Wan, M. *Adv. Funct. Mater*. **2003**, *13*, 925–928.
(15) (a) Xia, H. B.; Narayanan, J.; Cheng, D. M.; Xiao, C. Y.; Liu, X. Y.; Chan, H. S. O. *J. Phys. Chem. B* **2005**, *109*, 12677. (b) Zhang, L.; Peng, H.; Kilmartin, P. A.; Soeller, C.; Travas-Sejdic, J. *Macromolecules* **2008**, *41*, 7671–7678. (c) Zhang, X.; Chechik, V.; Smith, D. K.; Walton, P. H.; Duhme-Klair, A.-K. *Macromolecules* **2008**, *41*, 3417–3421. (d) Meng, L.; Lu, Y.; Wang, X.; Zhang, J.; Duan, Y.; Li, C. *Macromolecules* **2007**, *40*, 2981–2983.
(16) (a) Zhang, L.; Zujovic, Z. D.; Peng, H.; Bowmaker, G. A.; Kilmartin, P A.; Travas-Sejdic, J. *Macromolecules* **2008**, *41*, 8877–8884. (b) Anilkumar, P.; Jayakannan, M. *Macromolecules*

2008, *41*, 7706–7715. (c) Stejskal, J.; Sapurina, I.; Trchová, M.; Konyushenko, E. N. *Macromolecules* **2008**, *41*, 3530–3536. (d) Qiu, H.; Wan, M.; Matthews, B.; Dai, L. *Macromolecules* **2001**, *34*, 675–677. (e) Pan, L.; Pu, L.; Shi, Y.; Song, S.; Xu, Z.; Zhang, R.; Zheng, Y. *Adv. Mater.* **2007**, *19*, 461–464.

(17) (a) Kim, J. B.; Oh, G. S.; Han, G. M.; Im, S. S. *Langmuir* **2000**, *16*, 5841. (b) Kim, D.; Choi, J.; Kim, J.-Y.; Han, Y.-K.; Sohn, D. *Macromolecules* **2002**, *35*, 5314–5316.

(18) (a) Du, X.-S.; Zhou, C.-F.; Wang, G.-T.; Mai, Y.-W. *Chem. Mater.* **2008**, *20*, 3806–3808. (b) Ding, H.; Wan, M.; Wei, Y. *Adv. Mater.* **2007**, *19*, 465–469. (c) Zhao, M.; Wu, X.; Cai, C. *J. Phys. Chem. C* **2009**, *113*, 4987–4996. (d) Huang, J. X.; Kaner, R. B. *J. Am. Chem. Soc.* **2004**, *126*, 851.

(19) (a) Han, J.; Song, G.; Guo, R. *Adv. Mater.* **2007**, *19*, 2993–2999. (b) Zhou, C.; Han, J.; Guo, R. *Macromolecules* **2009**, *42*, 1252–1257. (c) Zhou, C.; Han, J.; Guo, R. *Macromolecules* **2008**, *41*, 6473–6479. (d) Zhou, C.; Han, J.; Song, G.; Guo, R. *Macromolecules* **2007**, *40*, 7075–7078. (e) G. Fu, D.; Zhao, J. P.; Sun, Y. M.; Kang, E. T.; Neoh, K. G. *Macromolecules* **2007**, *40*, 2271–2275.

(20) (a) Li, G.; Peng, H.; Wang, Y.; Qin, Y.; Cui, Z.; Zhang, Z. *Macromol. Rapid Commun.* **2004**, *25*, 1611–1614. (b) Yu, Q. Z.; Li, Y.; Wang, M.; Chen, H. Z. *Chin. Chem. Lett.* **2008**, *19*, 223–226.

(21) Bereket, G.; Hür, E.; Sahin, Y. *Appl. Surf. Sci.* **2005**, *252*, 1233–1244.

(22) Mandíc, Z.; Duíc, L.; Kovăčicek, F. *Electrochim. Acta* **1997**, *42*, 1389–1402.

(23) Zhang, H.; Wang, J.; Wang, Z.; Zhang, F.; Wang, S. *Synth. Met.* **2009**, *159*, 277–281.

(24) (a) Watanabe, A.; Mori, K.; Iwasaki, Y.; Nakamura, Y.; Niizuma, S. *Macromolecules* **1987**, *20*, 1793–1796. (b) Verghese, M. M.; Ramanathan, K.; Ashraf, S. M.; Kamalasanan, M. N.; Malhotra, B. D. *Chem. Mater.* **1996**, *8*, 822–824. (c) Mondal, S. K.; Barai, K.; Munichandraiah, N. *Electrochim. Acta* **2007**, *52*, 3258–3264. (d) Sine, G.; Hui, C. C.; Kuhn, A.; Kulesza, P. J.; Miecznikowski, K.; Chojak, M.; Paderewska, A.; Lewera, A. *J. Electrochem. Soc.* **2003**, *150*, C351–C355. (e) Guo, Y.; Zhou, Y. *Eur. Polym. J.* **2007**, *43*, 2292–2297. (f) Zhao, G.-Y.; Li, H.-L. *Microporous Mesoporous Mater.* **2008**, *110*, 590–594. (g) Zhao, X. Y.; Zang, J. B.; Wang, Y. H.; Bian, L. Y.; Yu, J. K. *Electrochem. Commun.* **2009**, *11*, 1297–1300. (h) Peng, X.-Y.; Luan, F.; Liu, X.-X.; Diamond, D.; Lau, K.-T. *Electrochim. Acta* **2009**, *54*, 6172–6177. (i) Dhawale, D. S.; Salunkhe, R. R.; Jamadade, V. S.; Gujar, T. P.; Lokhande, C. D. *Appl. Surf. Sci.* **2009**, *255*, 8213–8216. (j) Jugović, B.; Gvozdenović, M.; Stevanovićc, J.; Trišovića, T.; Grgur, B. *Mater. Chem. Phys.* **2009**, *114*, 939–942.

(25) Aoki, K.; Tano, S. *Electrochim. Acta* **2005**, *50*, 1491–1496.

(26) Mallick, K.; Witcomb, M.; Dinsmore, A.; Scurrell, M. S. *Macromol. Rapid Commun.* **2005**, *26*, 232–235.

(27) Zhang, X.; Goux, W. J.; Manohar, S. K. *J. Am. Chem. Soc.* **2004**, *126*, 4502–4503.

(28) Cao, Y.; Mallouk, T. E. *Chem. Mater.* **2008**, *20*, 5260–5265.

(29) Kotz, R.; Carlen, M. *Electrochim. Acta* **2000**, *45*, 2483–2498.

(30) Prasad, K.; Miura, N. *J. Power Sources* **2004**, *135*, 354–360.